VNUHCM Journal of Engineering and Technology 2026, 9(2):2859-2871

Open Access Full Text Article

Research Article

Research on establishing form error predictive model for Al6061 spherical surfaces in ultra-precision turning using artificial neural network

Do Manh Tung, Chu Anh My, Duong Xuan Bien*, Nguyen Kim Hung, Hoang Nghia Duc, Bui Kim Hoa, Ngo Viet Hung

ABSTRACT

Currently, driven by the increasing demand for precision in optical and mechanical components, complex surfaces are now required to maintain profile errors within micrometric tolerances. The development of profile error prediction models is, therefore, not merely a technical solution but a vital instrument for optimizing product quality, enhancing cost-effectiveness, minimizing scrap rates, and streamlining machining lead times. This study presents a predictive model for the form error of spherical surface (SS) on Al6061 aluminum alloy during ultra-precision turning (UPT) using a single-crystal diamond tool. The prediction model was developed based on a back-propagation (BP) neural network (NN) structure. The dataset for establishing the prediction model was collected from 30 precision machining experiments on spherical surfaces. To ensure the objectivity and reliability of the data, the fixturing and alignment procedures as well as the measurement method for profile error were standardized and thoroughly modeled. The cutting parameters, including spindle speed (n – rev/min), feed rate (F - mm/min), and depth of cut (ap - μm), were identified as independent variables to establish the relationship with the profile error. The determination of the appropriate neuron ratio between layers was investigated through six specific network structures. The criteria for evaluating the prediction quality of the neural network included the coefficient of determination (R^2), mean squared error (MSE), and mean absolute percentage error (MAPE). Accordingly, the artificial neural network ANN structure 3:5:20:1 delivered the best prediction performance, achieving an R^2 value of 1, MSE of 26.9, RMSE of 5.19, and MAPE of 0.2%. The results not only confirm the effectiveness of the proposed method but also provide a reliable scientific foundation for the development of profile error prediction models. At the same time, this study demonstrates the potential for extending the application to other complex surfaces such as aspheric surfaces, diffractive surfaces, or on different substrate materials.

Key words: Ultra-Precision Turning, Spherical surface, Form error, Neural Network

University of Le Quy Don, Ha Noi, Viet Nam

Correspondence

Duong Xuan Bien, University of Le Quy Don, Ha Noi, Viet Nam

Email: duongxuanbien@lqdtu.edu.vn

History

- Received: 22-05-2025
- Revised: 11-06-2025
- Accepted: 17-04-2026
- Published Online: 02-06-2026

DOI :
https://doi.org/10.32508/vnuhcmj-et.v9i2.1518

Check for updates

INTRODUCTION

Ultra-precision machining (UPM) technology is an achievement from the combination of modern technology and advanced mechanical processing technology to improve machining accuracy. UPM technology forms several types, including super-precision cutting, super-precision grinding, and super-precision special machining [1]. Currently, UPM is a development direction of modern manufacturing with products with micrometer and nanometer level precision [2]. UPT is one of the UPM methods mentioned above and it is used to machine parts with high roughness and form accuracy of SS [3,4]. UPT is applied in fields such as medicine, aerospace, military, and automobiles [5]. In particular, UPT is also applied in the field of optical lens manufacturing and lens mold [6–8]. Optical lenses with SS are a popular type of lens, widely used in the field of optics, leading to the need for lens production to be of interest and research. The spherical mold used to cast lenses [9] has a spherical surface created by a tool path that is a circular curve.

Optical lens technical criteria are evaluated by size tolerance, roughness surface, in addition to a very important criterion, form error (FE) [10,11]. In the optical glass manufacturing industry, form accuracy requirements are considered an extremely important issue because it directly affects optical performance, light beam precision and resolution. To ensure that optical lenses have high precision, require minimal machining, and enhance both efficiency and quality of manufacturing, the optical lens molding molds must have as high precision as possible. Copper parts FE with SS is considered in [9] with the evaluation of the influence from cutting tool deflection during the UPT process.

Cite this article : Manh Tung D, Anh My C, Xuan Bien D, Kim Hung N, Nghia Duc H, Kim Hoa B, Viet Hung N. **Research on establishing form error predictive model for Al6061 spherical surfaces in ultra-precision turning using artificial neural network**. *VNUHCM J. Eng. Technol.* 2026; 9(2):2859-2871.

A method to improve the lens casting process by improving the mold form accuracy in machining on an UPT is described in [7].

In recent years, with the development of computer science, artificial neural networks (ANN) have become a popular choice in building predictive models. The biggest advantage of artificial neural networks is their ability to effectively model linear or nonlinear and complex relationships between multiple input factors (3 input parameters: spindle speed, cutting depth, feed rate) and output parameters (1 parameter: profile error) [12]. These are relationships that are difficult or impossible to fully represent with traditional mathematical models. Developing a neural network often requires a complete data set to ensure the training process and produce results that can generalize well to the input data [13]. In addition, ANN also have the ability to respond appropriately to different types of input data, demonstrating high flexibility and adaptability to complex problems [14]. Although ANN has many advantages, there are still some notable disadvantages such as overfitting (when the model only remembers the provided data). However, some features can be adjusted in the network to optimize the neural network, making it suitable for solving problems in the mechanical field (the problems are often nonlinear and complex). M. O. Okwu et al. [13] built an ANN network model in predicting surface roughness in the drilling process. The effectiveness and reliability of ANN in establishing prediction models are also compared with other prediction models and presented in detail in [15]. Artificial intelligence networks include forward propagation networks [16], BP networks [12], and convolutional networks [15]. The back propagation (BP) network model is popular and widely used because of its superiority and high accuracy [17]. Additionally, using Gradient Descent technique in the BP network improves prediction accuracy [18,19]. Specifically, the BP network has been applied and presented in predicting the material removal rate when turning Al6061 alloy [20]. Establishing a model to predict surface quality [21] in turning stainless steel.

In practice, there are many regression methods to develop predictive models for form error, such as Response Surface Methodology (RSM) (including Box-Behnken and Central Composite Design models), the Taguchi method, Grey regression, multivariate regression, Genetic Programming, and Artificial Neural Networks (ANN). Each method has its own advantages and disadvantages, and ANN is no exception. The reason this study employs neural networks is due to several reasons as follows:

(1) The type of machining in this study is ultra-precision machining, about which little knowledge has been published, especially regarding the influence of cutting parameters on the objective functions (form error, surface roughness).

(2) When using popular regression methods such as RSM, Taguchi, and Grey, the results evaluating the influence of each parameter or parameter pair on the objective function show complex and hard-to-control characteristics or fail to fully describe the relationships between variables. These regression models are generally accurate for most conventional machining processes but are limited by the type of predictive model (first- or second-order models). Using higher-order predictive models may still fail to accurately capture the underlying nature or lead to non-convergent predictions. These issues are also present in ultra-precision machining.

(3) ANN models do not depend on the form of the regression equation but only on the nature of input data, the activation functions, and the appropriate network structure (number of layers or number of neurons in each hidden layer). Many previous studies have shown that ANN can effectively describe nonlinear and complex relationships between input factors and output parameters. In practice, training ANN with experimental input datasets has yielded promising results and demonstrated high accuracy in predicting form error values, as presented in this research.

This article focuses on establishing a model to predict form accuracy in ultra-precisely turning an Al6061 spherical mold with a diamond tip through the investigation of ANN structures. These network structures have a fixed number of layers, the number of neurons in each layer varied according to a specific ratio. The most suitable BP network structure is selected based on the criteria of suitability and accuracy. The evaluation and comparison results can be used as a basis for establishing similar network structures in the future.

RESEARCH CONTENT

Experimental setup

The entire experiment was performed on a Nanoform® X ultra-precision diamond lathe (Fig. 1). The Al6061 billet has a height of 20mm, an outer diameter of 30mm and a sphere radius of 19.5mm. FE were measured with the Form Talysurf ® i-Series PRO instrument (Fig. 2). This device is a highly precise measurement instrument utilized for assessing FE in spherical, aspherical, and diffractive surfaces. It has a measuring range of up to 20mm and a resolution of up to 0.2 nm.

The chemical composition of the workpiece material is presented in Tab. 1. Fig. 3 depicts some spherical blanks used for UPT machining.
Diamond turning tool NN60R0635mWGC-MS0454 has basic parameters including tip radius of 0.649 mm, front angle of - 250, rear angle of 100, cutting height of 7.475mm, tool tip material of natural diamond. The cutting tool parameters are described specifically in Fig. 4.

Figure 1: Ultra-Precision Turning Machine Nanoform® X [Source: Authors]

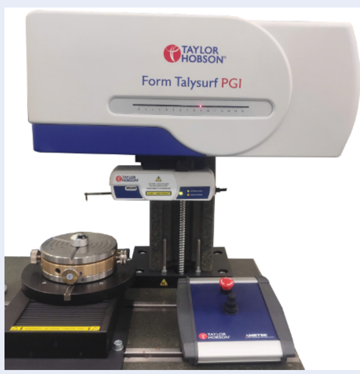

Figure 2: Form Talysurf® Measurement Machine [Source: Authors]

Figure 3: Al6061 Spherical Workpiece [Source: Authors]

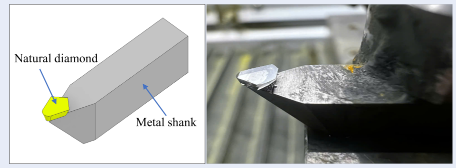

Figure 4: Diamond tool [Source:Authors]

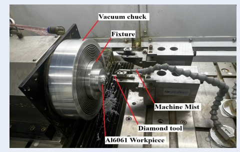

Figure 5: Machining system [Source: Authors]

Fig. 5 depicts the technological system including a UPT machine with vacuum chuck, fixture, spherical blank and diamond cutting tool. A mist coolant spray system is used simultaneously to continuously blow away chips to avoid leaving scratches on the product surface.
The experiments were conducted with different cutting modes and within the recommended range from the cutting tool supplier, the capabilities of the UPT machine and through some preliminary experiments. The experimental matrix used to design experiments is established according to the Box-Berken experimental model and Center Composite Design. These two models are typically used in many different studies[22]. They help reduce the number of experiments while still providing complete information and accurate assessment of factors affecting product quality. The total number of experiments is 30 and the range of experimental values is described in Tab. 2. The specific values of the experiments are described in detail in Tab. 7.

Research calibration

In order to obtain the experimental results for this research, the following calibration procedures were implemented: (1) the machine calibration procedure, (2) the measurement equipment calibration procedure, and (3) the measurement data processing procedure. First, the calibration procedure for the ultra-precision lathe is described in the diagram shown in Fig.6 below. It should be noted that Steps 3 and 4 are the most critical, as they have a direct impact on the FE of the SS. The runout correction process (Step 3) is performed by using a rubber hammer to compensate for the asymmetry error about the spindle axis. The

Table 1: Chemical composition of Al6061 [21]

No.	Mg	Si	Mn	Ti	Z	Cu	Fe	Cr	Al
wt.%	0.8-1.2	0.4-0.8	0.15	0.15	0.25	0.15-0.4	0.7	0.04-0.35	Balance

Table 2: Limit the range of experimental parameter values [Source: Authors]

Cutting parameters	Minimum value	Maximum value	Low level (-1)	Basic level (0)	High level (+1)	Vari-ables
n (rev/min)	823.44	2176.56	1000	1500	2000	x1
F (mm/min)	1.47	28.53	5	15	25	x2
ap (μm)	0.9406	9.06	2	5	8	x3

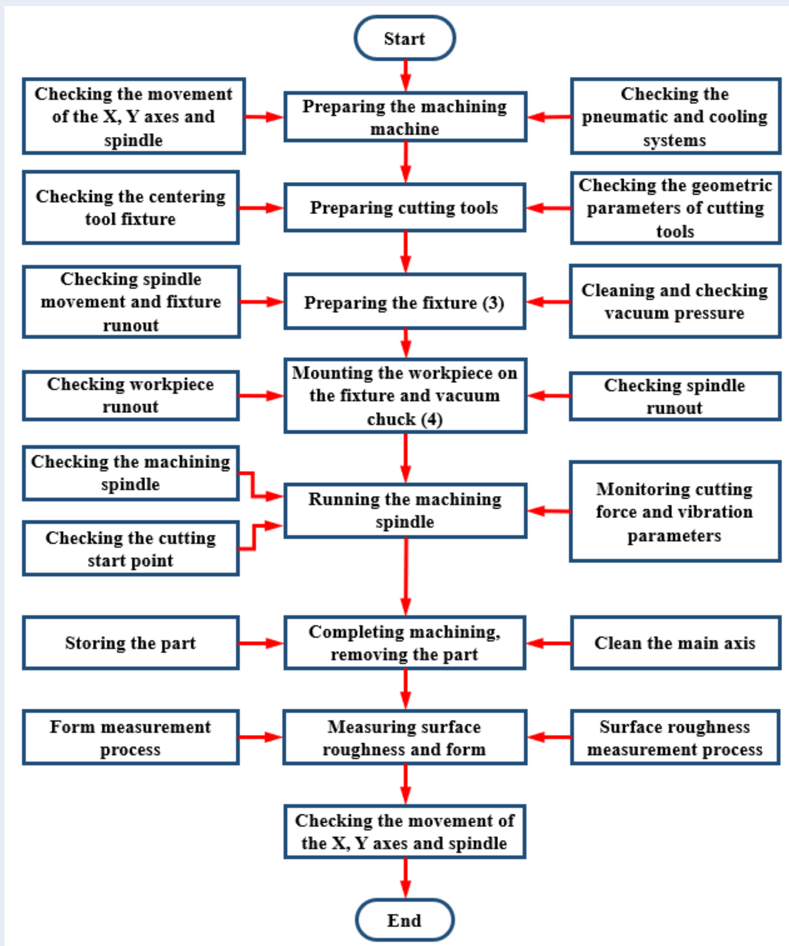

Figure 6: Ultra-precision lathe calibration diagram [Source: Authors]

workpiece runout is displayed on the UPT machine screen. The operator adjusts the workpiece based on the error shown on the machine, as illustrated in Fig.7.

Figure 7: Workpiece runout adjustment (Step 3) [Source: Authors] *(a) workpiece runout adjustment; (b) workpiece runout display screen*

The spindle runout correction process (Step 4) is performed automatically and is integrated into the UPT machine system. The operator plays a role in adjusting measurement parameters such as spindle speed, expected feed rate, and runout compensation by tuning the set screws on the chuck. The adjustment process and its results are illustrated in Fig.8.

Figure 8: Spindle runout correction (Step 4) [Source: Authors] *(a) spindle dynamic runout adjust-ment; (b) spindle dynamic runout display screen*

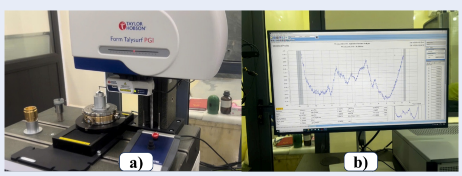

Figure 9: Calibration and setup of the measuring [Source: Authors] *(a) adjustment and setup of the FE measurement system; (b) FE results display screen*

Fig.9 illustrates the measuring device and the actual measurement results of the spherical surface form error. (2) The calibration diagram of the measurement process for spherical surface form error is shown in Fig.10.

(3) Measurement data calibration

The measurement data obtained from the experiments will be normalized using the data normalization technique before being fed into the neural network training. This process is necessary for data with different units and scales to bring the data onto a common value range. Calibration helps prevent imbalance and bias toward factors with larger absolute values during training. In particular, the calibration process improves the convergence speed of the ANN training, reduces errors during network propagation, and enhances the stability and accuracy of the model. The normalization method used is Min-Max normalization, which scales all values to the range [0, 1] according to the formula:

$$x_{norm} = \frac{x - x_{min}}{x_{max} - x_{min}}$$

Where, x is the original value of the input or output variable; x_{min} is the minimum value in the dataset of that variable; x_{max} is the maximum value in the dataset of that variable x_{norm} is the value after normalization.

Artificial neural network model

The BP network model is built through the differentiation of the loss function from the last layer back to the first layer to continuously adjust the coefficients b_i and w_i accordingly [12,15,20,23]. The last layer is computed first because its value is close to the expected output level. Calculating the derivative for previous layers is done based on the "Chain rule". The derivative is calculated step by step for the objective function and the algorithm stops when the loss function reaches its minimum value or the number of iterations is limited. The steps to implement the algorithm can be illustrated as shown in Fig. 11.

One of the advantages of the BP network is to avoid the phenomenon of high bias. This is the phenomenon in which the optimal set of parameters is found too quickly and satisfies the global optimal value. At this point, the entire algorithm loop in the BP network only receives a single set of values. That makes the ANN network not reliable enough to draw conclusions. However, the disadvantages of this method become apparent when the ANN structure is complex. Accordingly, calculating the loss function also becomes quite complicated.

The R2 [15], MSE [24], RMSE [7] and MAPE [25] indexes are used to assess the quality and suitability in training NN. Those indicators are described specifically in Tab. 3 where is the measured value from experiments; is the predicted value; n is the total number of experiments.

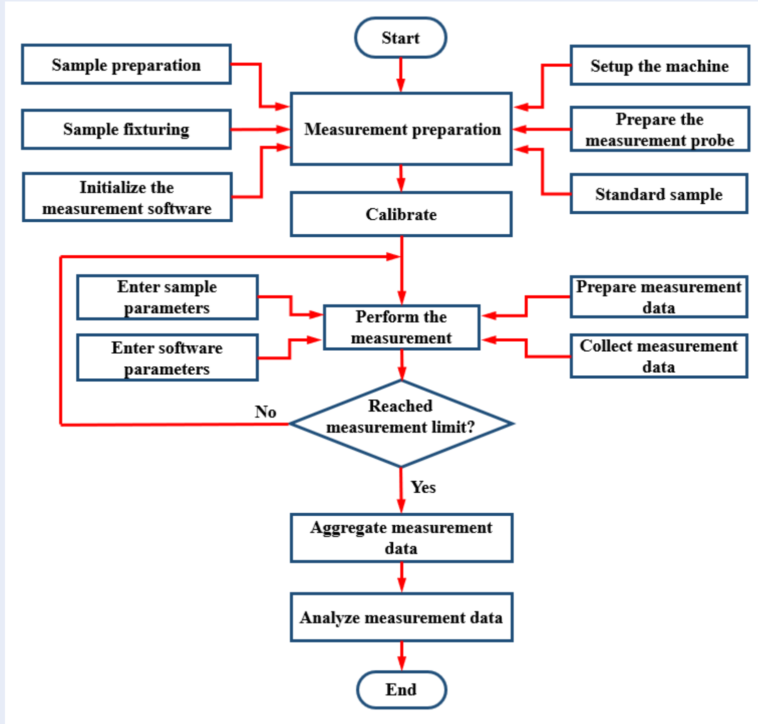

Figure 10: Calibration process of measuring surface formerror [Source: Authors]

Table 3: Model evaluation criteria. [7,15,24,25]

No.	Indexs	Formula	Significances
1	R2	$R^2 = 1 - \left\| \frac{\sum_{i=1}^{n} (y_i - \widehat{y}_i)^2}{\sum_{i=1}^{n} (\widehat{y}_i)^2} \right\|$	Evaluate the appropriateness of the regression model
2	MSE	$MSE = \frac{1}{n} \sum_{i=1}^{n} (y_i - \widehat{y}_i)^2$	Assessment the accuracy of the prediction model. The smaller the value, the more accurate it is
3	RMSE	$RMSE = \sqrt{\frac{1}{n} \sum_{i=1}^{n} (y_i - \widehat{y}_i)^2}$	
4	MAPE	$MAPE = 100.\frac{1}{n} \sum_{i=1}^{n} \left(\frac{\|y_i - \widehat{y}_i\|}{\widehat{y}_i} \right)$	Evaluate the deviation of predicted values from actual values, calculated in percentage.

Calculation results and discussion

The BP network is designed with an input layer of 3 variables including cutting speed (n - rev/min), feed speed (F - mm/min), depth of cut (ap - μm). The output layer is the deformation error value (PV - nm). Some studies such as [26,27] have evaluated the suitability and accuracy of NN through changing the structure. Combined with some experiments using an ANN with three input variables, the number of neurons in the first hidden layer is chosen to be five, which yields correct results and high accuracy [28]. The basic parameters of the BP network are presented specifically in Tab. 4.

With the number of neurons in hidden layer 1 of the NN fixed and the ratio of neurons between hidden layers changing specifically as follows: (1:1), (1:2), (1:3), (1:4), (1:5), and (1:6) correspond to the structures specifically described in Tab. 5. Results of BP network quality assessment corresponding to the cases for all data are expressed through specific indicators. These metrics are computed based on the congruence between empirical data and predicted outcomes

All 6 network models have an R^2 index approaching 1 and equal to 1. This shows that the prediction models have a very high level of agreement with actual data. The indicators of prediction accuracy such as MAPE,

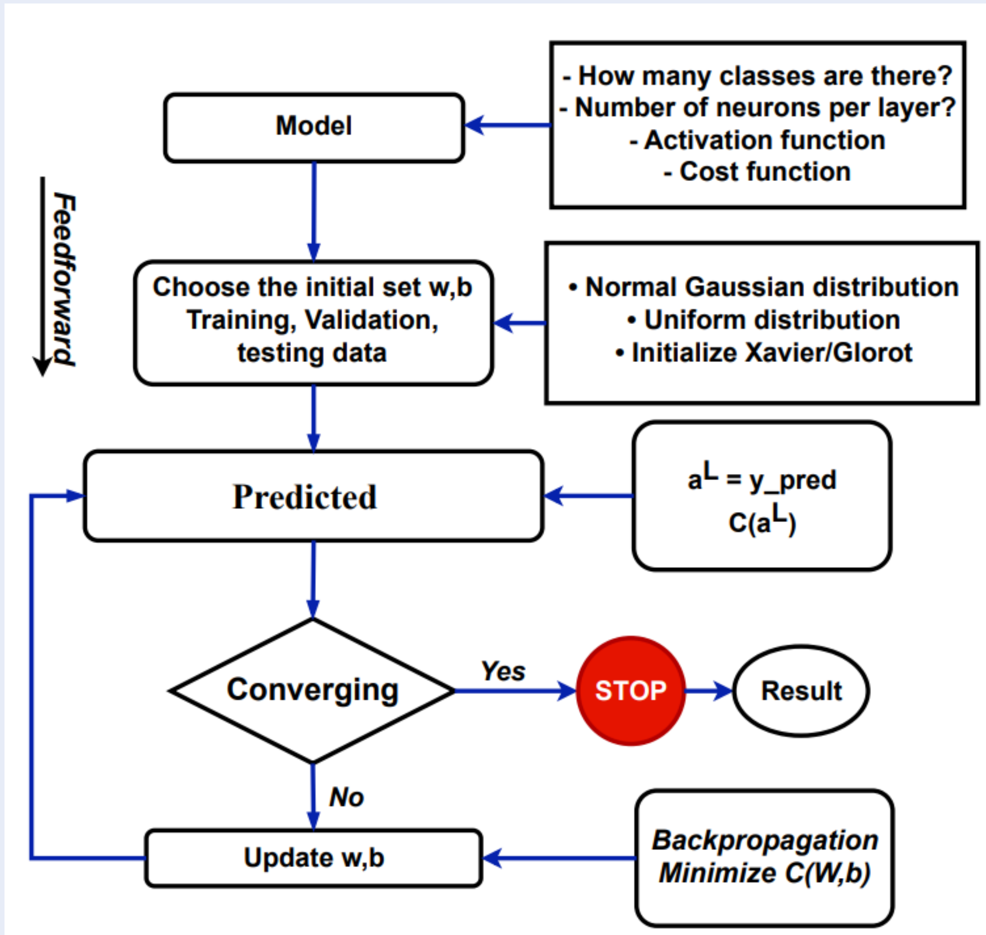

Figure 11: Diagram of BP neural network [Source: Authors]

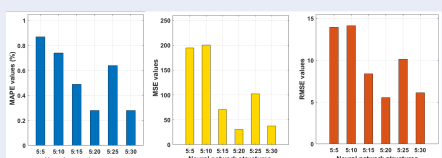

Figure 12: MAPE, MSE, RMSE values correspond tostructural ratios [Source: Authors]

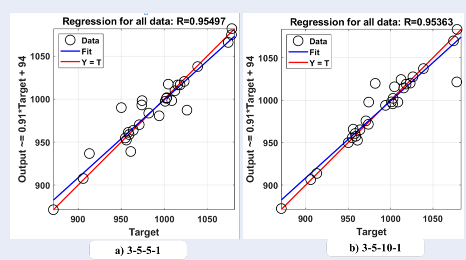

Figure 13: Regression value of network structures 3-5-5-1(a) và 3-5-10-1 (b) [Source: Authors]

MSE, RMSE show differences between models. The bar charts in Fig. 12 compare the MAPE, MSE, and RMSE values with those in Tab. 5. The training results of NN with different structures are also shown through regression models as depicted in Fig. 13, Fig. 14 and Fig. 15.

The regression chart shows that the performance and fit of each structure with the entire data are high, all regression results have R > 0.95. Through the results obtained, the 3-5-20-1 structure corresponding to the ratio of the number of neurons between layers of 1:4 gives the highest regression index of the prediction model with experimental data (R = 0.993) (Fig. 14b). Based on the criteria described in Fig. 12 and the R regression charts in Fig. 13, Fig. 14 and Fig. 15,

Table 4: BP network structure parameters [Source: Authors]

No.	BP network parameters	Value
1	Number of input layer variables	3
2	Number of output layer variables	1
3	Number of hidden layer neurons 1	5
4	Number of hidden layer 2 neurons (in 6 different scales)	Tab. 5
5	Data sharing ratio: Training / Validation/ Test	80%/10%/10%
6	Number of experiments	30
7	Transfer function	Logsig
8	Training function	traingdx
9	Number of training iterations (Maximum number of epochs to train)	20000
10	Fitness function	MSE
11	Learning rate	0.01
12	Ratio to increase learning rate	1.05
13	Ratio to decrease learning rate	0.8
14	Momentum constant	0.9

Table 5: Structure table and calculation results of R^2, MSE and MAPE indicators [Source: Authors]

Network structure	R2			MSE			MAPE(%)			RMSE		
	Train	Test	All data	Train	Test	All data	Train	Test	All data	Train	Test	All data
5-5	0.99	0.99	0.99	157.75	520.0	194.66	0.80	1.47	0.87	12.56	22.80	13.95
5-10	0.99	0.99	0.99	107.85	1068	200.23	0.60	1.93	0.74	10.39	32.68	14.15
5-15	0.99	1.00	0.99	81.58	2.192	70.40	0.54	0.12	0.49	9.03	1.48	8.39
5-20	1.00	1.00	1.00	35.43	15.72	30.95	0.28	0.33	0.28	5.95	3.97	5.56
5-25	0.99	1.00	0.99	107.83	10.94	102.34	0.65	0.25	0.64	10.38	3.31	10.12
5-30	1.00	1.00	1.00	46.956	0.641	37.67	0.33	0.07	0.28	6.85	0.80	6.14

the structure 3-5-20-1 gives the best prediction results (Fig. 17). Training the BP neural network not only on the choice of program structure but also on the number of times the program is newly trained. At each training session, the value set serving the processes "Training", "Validation" and "Test" is randomly selected at a ratio of 80% :10% :10% respectively. This leads to different results at each activation. That demonstrates the objectivity of the process of establishing and choosing the network structure. The 3-5-20-1 structure went through 6 consecutive runs to select the most optimal data set and the survey results are shown in Tab. 6.

The survey results between model training activations are also visually depicted in Fig. 12. From Tab. 6 and Fig. 17, through the R^2, MSE, RMSE and MAPE indices, we see that the 4th run gives the best results with a regression index on the entire data of R = 0.994 and a regression index on the training data is R = 0.993 which is clearly shown in Fig. 18.

Table 6: Indicators R^2, MSE, RMSE and MAPE ofthe 3-5-20-1 structure [Source: Authors]

Number of runs	R2			MSE			MAPE(%)			RMSE		
	Train	Test	All data	Train	Test	All data	Train	Test	All data	Train	Test	All data
1	1.00	1.00	1.00	35.43	15.72	30.95	0.28	0.33	0.28	5.95	3.97	5.56
2	0.99	0.99	0.99	88.77	93.53	88.25	0.67	0.69	0.66	9.42	9.67	9.39
3	0.99	0.99	0.99	147.05	192.01	153.43	0.89	1.10	0.91	12.13	13.86	12.39
4	1.00	1.00	1.00	33.37	1.6454	26.90	0.23	0.09	0.20	5.78	1.28	5.19
5	1.00	1.00	1.00	34.10	4.99	27.79	0.25	0.12	0.22	5.84	2.23	5.27
6	1.00	1.00	1.00	36.27	0.03	29.19	0.29	0.01	0.24	6.02	0.16	5.40

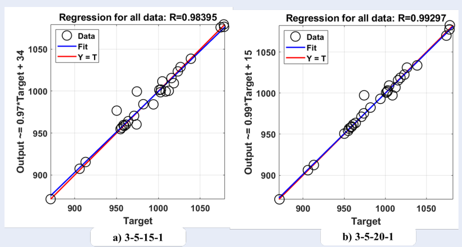

Figure 14: Regression value of network structures 3-5-15-1 (a) và 3-5-20-1 (b) [Source: Authors]

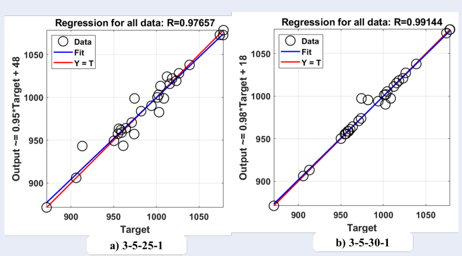

Figure 15: Regression value of network structures 3-5-25-1 (a) và 3-5-30-1 (b) [Source: Authors]

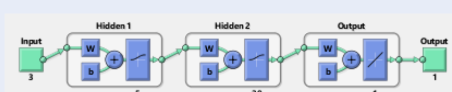

Figure 16: The structure illustrates the 3-5-20-1 network [Source: Authors]

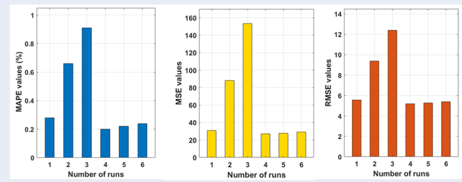

Figure 17: MAPE, MSE, RMSE values of 3-5-20-1 during training sessions [Source: Authors]

Tab. 7 shows the experimental results of actual FE (FE_ex) and prediction FE (FE_pre) results with the 3-5-20-1 structure and the difference value (%) between them. Fig. 19a depicts the SS form error between the experimental measurement results and the predicted value in Tab. 7.

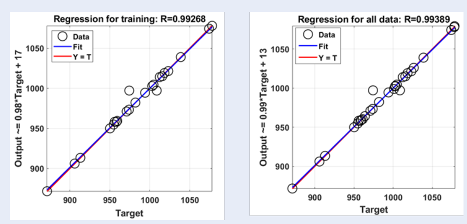

Figure 18: Regression value of network structure 3-5-20-1 at the 4th run [Source: Authors]

Fig. 19b shows the difference between the predicted value and the actual value. Those difference values are all very small and close to 0. There are only 3 cases with error values from 1.1% to 2.3%, in experiment number 13, 14, 15. The remaining cases show very high prediction accuracy with a difference of less than 0.3%.

Table 7: Compare predicted results and actual results [Source: Authors]

No.	(rev/min)	F (mm/min)	ap (μm)	FE_ex (nm)	FE_pre (nm)	Difference (%)
1	1000	5	5	1001.1	998.90	0.220
2	2000	5	5	1003.0	1002.85	0.015
3	1000	25	5	1038.8	1038.99	0.018
4	2000	25	5	1023.2	1021.54	0.162
5	1000	15	2	1015.6	1015.08	0.051
6	2000	15	2	1078.1	1078.02	0.007
7	1000	15	8	1074.3	1074.37	0.007
8	2000	15	8	973.9	973.37	0.054
9	1500	5	2	959.2	959.36	0.017
10	1500	25	2	1002.5	1002.24	0.026
11	1500	5	8	961.1	960.23	0.091
12	1500	25	8	950.2	950.00	0.021
13	1500	15	5	1008.7	997.16	1.144
14	1500	15	5	1008.7	997.16	1.144
15	1500	15	5	974.3	997.16	2.346
16	1000	5	2	871.3	871.60	0.034
17	2000	5	2	958.3	958.19	0.011
18	1000	25	2	905.9	906.12	0.024
19	2000	25	2	982.0	982.23	0.023
20	1000	5	8	956.0	958.20	0.230
21	2000	5	8	913.1	913.31	0.023
22	1000	25	8	1026.4	1026.01	0.038
23	2000	25	8	1018.4	1019.08	0.067
24	823	15	5	1078.5	1079.22	0.067
25	2177	15	5	1004.7	1004.49	0.021
26	1500	2	5	954.8	954.82	0.002
27	1500	29	5	964.0	964.19	0.020
28	1500	15	1	971.0	971.08	0.008
29	1500	15	9	994.1	994.48	0.038
30	2000	15	5	1012.4	1014.03	0.161

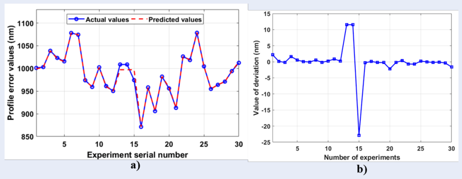

Figure 19: Predicted vs. measured values (a) and their deviation (b) [Source: Authors]

CONCLUSIONS

Ultra-precise turning of lens surfaces (spherical, aspherical, diffractive) in general and SS in particular is being strongly developed in some countries with advanced science such as the US, UK, China, India and Japan. Although the potential applications of ultra-precision surfaces have been proven in many different important fields, the issue of mastering UPM equipment and technology is still a hot issue and many challenges. This article has approached UPT technology in the direction of experimental research with quality control of typical SS machining. This is the base surface for different types of lens surfaces as well as their various applications.

The NN was chosen as the research object to establish a model to predict spherical FE Al6061. This choice is suitable for reality because UPM technology as well as high-speed machining technology have many differences compared to traditional machining methods. Controlling quality factors at the micrometer or nanometer level is truly a big challenge. Therefore, choosing a NN prediction model is most appropriate.

Accordingly, with 3 inputs and 1 output in 30 experiments, along with the survey of 06 NN models, this study has identified a 3-5-20-1 structure corresponding to the ratio of neurons between two hidden layers of 1:4 that are most suitable in structures. The reliability of the model is confirmed based on 04 quality indicators with 2 levels of evaluation. Level 1 is to evaluate between structures to choose the most appropriate ratio of 1:4 (R^2 = 1, MSE = 30.95, RMSE = 5.56, MAPE = 0.28%). Level 2 is to assess the 3-5-20-1 structure between different training times due to the random nature of data set selection in the processes.

The results of this research are directly applied in predicting and controlling Al6061 spherical surface FE in UPT machining.

For spherical surfaces, the main geometric difference lies in the radius size of the sphere. The quality criteria include the spherical form error, surface roughness, and the radius dimension. Therefore, considering only the geometric aspect, this study can be fully applied to all spherical surfaces with different radii but made from the same type of material. Up to now, there are virtually no limitations regarding the geometric factors of spherical surfaces.

At the same time, it also has important value in establishing models to predict other surface quality factors such as roughness, dimensional errors or other criteria.

ABBREVIATIONS

UPM: Ultra-precision machining
SS: Spherical surface
UPT: Ultra-precision turning
BP: Back-propagation
ANN: Artificial neural networks
FE: Form Error
NN: Neural network
MSE: Mean squared error
MAPE: Mean absolute percentage error
RMSE: Root mean squared error
RSM: Response Surface Methodology

COMPETING INTERESTS

There are no potential conflicts of interest with respect to the research, authorship, and publication of this article.

AUTHORS' CONTRIBUTIONS

Duong Xuan Bien and Chu Anh My participated in coming up with writing ideas and reviewing the article.

Do Manh Tung and Ngo Viet Hung contributed to experimental design and data processing.

Nguyen Kim Hung collected the data and wrote the manuscript.

Bui Kim Hoa and Hoang Nghia Duc contributed to data interpretation.

ACKNOWLEDGEMENTS

This research is funded by Vietnam National Foundation for Science and Technology Development (NAFOSTED) under grant number 107.01-2020.15.

REFERENCES

1. Yaping F. Research of ultra precision machining technology. Applied Mechanics and Materials. 2014;687-691:476–9. Available from: https://doi.org/10.4028/www.scientific.net/AMM.687-691.476.
2. Olaniyan T, Faisal N, Njuguna J. Recent Developments in Mechanical Ultraprecision Machining for Nano/Micro Device Manufacturing. Micromachines. 2024;15(8):1030. Available from: https://doi.org/10.3390/mi15081030.
3. Tauhiduzzaman M, Yip A, Veldhuis SC. Form error in diamond turning. Precision Engineering. 2015;42:22–36. Available from: https://doi.org/10.1016/j.precisioneng.2015.03.006.

4. Zhang SJ, To S, Wang SJ, Zhu ZW. A review of surface roughness generation in ultra-precision machining. International Journal of Machine Tools; Manufacture. 2015;91:76–95. Available from: https://doi.org/10.1016/j.ijmachtools.2015.02.001.
5. Zhang Q, Guo N, Chen Y, Fu Y, Zhao Q. Simulation and Experimental Study on the Surface Generation Mechanism of Cu Alloys in Ultra-Precision Diamond Turning. Micromachines. 2019;10(9):573. Available from: https://doi.org/10.3390/mi10090573.
6. Xu Y, Du X, Wang Z, Liu H, Huang P, To S, et al. Room-Temperature Molding of Complex-Shaped Transparent Fused Silica Lenses. Advanced Science . 2023;10(34). Available from: https://doi.org/10.1002/advs.202304756.
7. Zhou T, Gao L, Yu Q, Wang G, Zhou Z, Yan T, et al. Machine learning for aspherical lens form accuracy improvement in precision molding of infrared chalcogenide glass. Precision Engineering. 2024;90:156–63. Available from: https://doi.org/10.1016/j.precisioneng.2024.08.007.
8. Zhou T, Zhu Z, Liu X, Liang Z, Wang X. A Review of the Precision Glass Molding of Chalcogenide Glass (ChG) for Infrared Optics. Micromachines. 2018;9(7):337. Available from: https://doi.org/10.3390/mi9070337.
9. Dai Y, Jiang J, Zhang G, Luo T. Forced-based deviation tool induce form error identification in single-point diamond turning of optical spherical surfaces. Precision Engineering. 2021;72:83–94. Available from: https://doi.org/10.1016/j.precisioneng.2021.04.001.
10. Evans CJ. Uncertainty evaluation for measurements of peak-to-valley surface form errors. CIRP Annals. 2008;57(1):509–12. Available from: https://doi.org/10.1016/j.cirp.2008.03.084.
11. Yu DP, Hong GS, Wong YS. Profile error compensation in fast tool servo diamond turning of micro-structured surfaces. International Journal of Machine Tools; Manufacture. 2012;52(1):13–23. Available from: https://doi.org/10.1016/j.ijmachtools.2011.08.010.
12. Kant G, Sangwan KS. Predictive Modelling and Optimization of Machining Parameters to Minimize Surface Roughness using Artificial Neural Network Coupled with Genetic Algorithm. Procedia CIRP. 2015;31:453–8. Available from: https://doi.org/10.1016/j.procir.2015.03.043.
13. Okwu MO, Otanocha OB, Edward BA, Oreko BU, Oyekale J, Oyejide OJ, et al. Investigating the Accuracy of Artificial Neural Network Models in Predicting Surface Roughness in Drilling Processes. Procedia Computer Science. 2024;232:1982–90. Available from: https://doi.org/10.1016/j.procs.2024.02.020.
14. Liu Q, Altintas Y. On-line monitoring of flank wear in turning with multilayered feed-forward neural network. International Journal of Machine Tools; Manufacture. 1999;39(12):1945–59. Available from: https://doi.org/10.1016/S08906955(99)00020-6.
15. Bello O, Holzmann J, Yaqoob T, Teodoriu C. Application Of Artificial Intelligence Methods In Drilling System Design And Operations: A Review Of The State Of The Art. Journal of Artificial Intelligence and Soft Computing Research. 2015;5(2):121–39. Available from: https://doi.org/10.1515/jaiscr-2015-0024.
16. García-Pérez A, Ziegenbein A, Schmidt E, Shamsafar F, Fernández-Valdivielso A, Llorente-Rodríguez R, et al. CNN-based in situ tool wear detection: A study on model training and data augmentation in turning inserts. Journal of Manufacturing Systems. 2023;68:85–98. Available from: https://doi.org/10.1016/j.jmsy.2023.03.005.
17. Ayyaswamy JP, Kulandaivel A, Ezilarasan C, Arunagiri A, Charles M, Kumar SR. Predictive model development in dry turning of Nimonic C263 by artificial neural networks. Materials Today: Proceedings. 2022;59(2):1284–90. Available from: https://doi.org/10.1016/j.matpr.2021.11.517.
18. Wu WY. A Back-Propagation Neural Network for Recognizing Object. European Journal of Engineering and Technology Research. 2022;7(5):102–9. Available from: https://doi.org/10.24018/ejeng.2022.7.5.2895.
19. Groenendijk R, Dorst L, Gevers T. Geometric Back-Propagation in Morphological Neural Networks. IEEE Transactions on Pattern Analysis and Machine Intelligence. 2023;45(11):14045–51.
20. Chaurasia VK, Kasdekar DK, Shivhare V. Development of Artificial Intelligence Model for the Prediction of MRR in Turning. International Journal of Hybrid Information Technology. 2016;9(2):75–82. Available from: https://doi.org/10.14257/ijhit.2016.9.2.07.
21. Gopal M. Prediction of surface roughness in turning of duplex stainless steel (DSS) using response surface methodology (RSM) and artificial neural network (ANN). Materials Today: Proceedings. 2021;47(pt19):6704–11. Available from: https://doi.org/10.1016/j.matpr.2021.05.118.
22. Aamir M, Tolouei-Rad M, Giasin K, Vafadar A. Machinability of Al2024, Al6061, and Al5083 alloys using multi-hole simultaneous drilling approach. Journal of Materials Research and Technology. 2020;9(5):10991–1002. Available from: https://doi.org/10.1016/j.jmrt.2020.07.078.
23. Sadhukhan B, Mondal NK, Chattoraj S. Optimisation using central composite design (CCD) and the desirability function for sorption of methylene blue from aqueous solution onto Lemna major. Karbala International Journal of Modern Science. 2016;2(3):145–55. Available from: https://doi.org/10.1016/j.kijoms.2016.03.005.
24. Miao L, Liao C, Zhang D, Liang H, Gao D. Optimization of milling parameters based on GA-BP neural network. Journal of Physics: Conference Series. 2024;2815(1). Available from: https://doi.org/10.1088/1742-6596/2815/1/012052.
25. Fan L, Ren Y, Tan M, Wu B, Gao L. GA-BP neural network-based nonlinear regression model for machining errors of compressor blades. Aerospace Science and Technology. 2024;151. Available from: https://doi.org/10.1016/j.ast.2024.109256.
26. Kim G, Yang SM, Kim DM, Choi JG, Lim S, Park HW. Developing a deep learning-based uncertainty-aware tool wear prediction method using smartphone sensors for the turning process of Ti-6Al-4V. Journal of Manufacturing Systems. 2024;76:133–57. Available from: https://doi.org/10.1016/j.jmsy.2024.07.010.
27. Mia M, Dhar NR. Prediction of surface roughness in hard turning under high pressure coolant using Artificial Neural Network. Measurement : Journal of the International Measurement Confederation. 2016;92:464–74. Available from: https://doi.org/10.1016/j.measurement.2016.06.048.
28. Guo Z, Xu C, Wang X, Feng P, Zhang M. Determination of tool tip steady-state temperature in dry turning process based on artificial neural network. Journal of Manufacturing Processes. 2022;79:600–13. Available from: https://doi.org/10.1016/j.jmapro.2022.05.021.

VNUHCM Journal of Engineering and Technology 2026, 9(2):2859-2871

Open Access Full Text Article

Bài nghiên cứu

Nghiên cứu xây dựng mô hình dự đoán sai số biên dạng bề mặt cầu Al6061 khi tiện siêu chính xác sử dụng mạng nơ ron nhân tạo

Do Manh Tung, Chu Anh My, Duong Xuan Bien*, Nguyen Kim Hung, Hoang Nghia Duc, Bui Kim Hoa, Ngo Viet Hung

TÓM TẮT

Hiện nay, trước yêu cầu ngày càng cao về độ chính xác của các chi tiết quang học và cơ khí chính xác, các chi tiết có bề mặt phức tạp đòi hỏi sai số biên dạng ở mức micromet. Việc phát triển các mô hình dự đoán sai số biên dạng không đơn thuần là một giải pháp kỹ thuật mà còn là công cụ quan trọng trong việc tối ưu hóa chất lượng sản phẩm, tối ưu chi phí, giảm tỷ lệ phế phẩm và giảm thời gian gia công. Nghiên cứu này trình bày mô quy dự đoán sai số biên dạng bề mặt cầu trên nền vật liệu hợp kim nhôm Al6061, khi tiện siêu chính xác (UPT) bằng mũi dao kim cương đơn tinh thể. Mô hình dự đoán được phát triển dựa trên cấu trúc mạng nơ ron lan truyền ngược (BPNN). Bộ dữ liệu để thiết lập mô hình dự đoán được thu thập từ 30 thí nghiệm gia công tinh bề mặt cầu. Để đảm bảo tính khách quan, tin cậy của dữ liệu, quy trình gá đặt điều chỉnh cũng như phương pháp đo lường kết quả sai số biên dạng đều đã được chuẩn hóa và mô hình hóa chi tiết. Các thông số cắt bao gồm tốc độ trục chính (n), tốc độ chạy dao (F) và chiều sâu cắt (ap) được xác định là các biến độc lập để thiết lập mối quan hệ với sai số biên dạng. Việc xác định tỉ lệ số nơ ron phù hợp giữa các lớp được khảo sát thông qua 06 cấu trúc mạng cụ thể. Các chỉ tiêu đánh giá chất lượng dự đoán của mạng nơ ron bao gồm chỉ số R^2, MSE và MAPE. Theo đó, cấu trúc ANN 3:5:20:1 cho kết quả dự đoán tốt nhất với chỉ số R^2 đạt 1, MSE là 26,9, RMSE là 5,19 và MAPE là 0,2%. Kết quả không chỉ khẳng định tính hiệu quả của phương pháp đề xuất mà còn cung cấp cơ sở khoa học đáng tin cậy trong việc phát triển các mô hình dự đoán sai số biên dạng. Đồng thời nghiên cứu này cũng cho thấy tiềm năng mở rộng áp dụng cho nhiều bề mặt phức tạp khác như bề mặt phi cầu, bề mặt nhiễu xạ hay trên các nền vật liệu khác nhau.

Từ khoá: tiện siêu chính xác, mặt cầu, sai số biên dạng, mạng nơ ron nhân tạo

Đại học Kỹ thuật Lê Quý Đôn, Hà Nội, Việt Nam

Liên hệ

Duong Xuan Bien, Đại học Kỹ thuật Lê Quý Đôn, Hà Nội, Việt Nam

Email: duongxuanbien@lqdtu.edu.vn

Lịch sử

- Ngày nhận: 22-05-2025
- Ngày sửa đổi: 11-06-2025
- Ngày chấp nhận: 17-04-2026
- Ngày đăng: 02-06-2026

DOI :
https://doi.org/10.32508/vnuhcmj-et.v9i2.1518

Trích dẫn bài báo này: Manh Tung D, Anh My C, Xuan Bien D, Kim Hung N, Nghia Duc H, Kim Hoa B, Viet Hung N. **Nghiên cứu xây dựng mô hình dự đoán sai số biên dạng bề mặt cầu Al6061 khi tiện siêu chính xác sử dụng mạng nơ ron nhân tạo**. *VNUHCM J. Eng. Technol.* 2026; 9(2):2859-2871.